Influence of Wind Tunnel Test Duration on Wind Load Factors

Dat Duthinh, M.ASCE[1]; Adam L. Pintar[2]; and Emil Simiu, F.ASCE[3]

Abstract: A method is presented for calculating the uncertainty associated with the estimation of peak pressure coefficients from wind tunnel test records of various lengths and how this uncertainty influences design wind effects. The proposed method is applicable to any type of structure and any type of civil engineering aerodynamic testing facility, including large-scale facilities. As an example of the application of the method, an investigation is presented of time series belonging to five categories of pressure coefficients implicit in Chapter 27 of the ASCE 7-10 Standard. The results of the investigation show that, for typical civil engineering wind tunnels, estimated design wind effects based on tests with durations as low as 10 s, corresponding to prototype durations of less than 6 min, are larger than their counterparts based on tests with 100 s duration by only approximately 5%. The proposed method provides useful indications on minimum lengths of pressure records to be measured in wind tunnels. **DOI: 10.1061/(ASCE)ST.1943-541X.0002202.**

Author keywords: Coefficient of variation; Extreme value distribution; Load factor; Peak-over-threshold; Pressure coefficient; Sampling error; Statistical independence; Uncertainty; Test duration; Wind tunnel test.

Introduction and Review

Wind load standards are based on wind tunnel tests and on safety margins founded on reliability concepts and calibration with respect to past practice. Time series of pressure coefficients measured in typical wind tunnels over a time interval T_m are used to estimate properties of the distribution of the peak pressure coefficients for time series of duration T_{1m}, where the subscript m stands for model, $T_{1m} \geq T_m$, and T_{1m} is the model counterpart of the prototype duration of a storm (i.e., 60 or 10 min, depending upon the building code being considered).

Wind tunnel operators are interested in recording time series over intervals T_m as short as possible, limited by the fact that the measured time series should include enough *independent* local peaks, from which extrapolation to longer time periods using extreme value analysis methods can produce reliable results. One limitation on the duration T_m is that the sampling error increases as the number of independent peaks decreases.

Minciarelli et al. (2001, conclusion #5, p. 10 and Section 4, p. 8) assumed either a normal or a Gumbel distribution of the peak wind effects and concluded from computer simulations that, "for low-rise buildings, increasing wind tunnel pressure record lengths beyond 20 or 30 min to obtain better estimates of peaks does not appear to improve significantly estimates of overall wind effects," but recommended further investigation "by considering other statistics of fluctuating time histories." Rofail and Kwok (1992) investigated various methods to obtain peak factors for wind effects and concluded that sample lengths can be reduced from one hour to 30 min without significantly affecting uncertainties.

The ASCE 7-10 Standard (ASCE 2010) in effect classifies pressures on buildings in five basic categories with specific spectral properties: pressures on interior, edge, and corner areas of roofs; and interior and edge areas of walls. In this work, records for individual taps belonging to each of the five categories are analyzed for two buildings. Conclusions based on these records with respect to the minimum acceptable record length are based on the worst case being considered (e.g., an individual tap at wall edge under the most demanding wind direction), and are therefore conservative. Their conservatism is stronger if they are applied to areas tributary to more than one tap, since owing to imperfect spatial correlation, the variability of the fluctuating pressures tends to decrease as the areas being considered are larger. The procedure developed in this note is therefore viewed as an appropriate basis for the estimation of minimum acceptable record lengths.

The design wind effects are functions of micrometeorological, aerodynamic, and wind climatological parameters. Because these parameters are affected by uncertainties, so will the design wind effects. This work considers these uncertainties, including, in particular, the dependence of the uncertainty in the peak pressure coefficient upon the time intervals T_m and T_{1m}, and the extent to which this uncertainty affects the design wind effects.

The note is organized as follows. The framework used to assess the influence of uncertainties in the pressure coefficients on the design wind effect is presented first. A peaks-over-threshold (POT) approach to the estimation of the distribution of the peaks and associated uncertainties is then presented. Sampling errors are estimated as functions of record length for time histories of pressure coefficients measured for each of five distinct categories of records implicit in the ASCE 7-10 Standard. The extent to which the record length affects the design wind effect for each of those categories is evaluated next, and conclusions are presented on the basis of this evaluation.

[1]Research Structural Engineer, Engineering Laboratory, NIST, Gaithersburg, MD 20899 (corresponding author). Email: dduthinh@nist.gov

[2]Mathematical Statistician, Statistical Engineering Division, NIST, Gaithersburg, MD 20899. Email: adam.pintar@nist.gov

[3]NIST Fellow, Engineering Laboratory, NIST, Gaithersburg, MD 2089. Email: emil.simiu@nist.gov

Note. This manuscript was submitted on August 1, 2017; approved on May 9, 2018; published online on August 17, 2018. Discussion period open until January 17, 2019; separate discussions must be submitted for individual papers. This technical note is part of the ***Journal of Structural Engineering***, © ASCE, ISSN 0733-9445.

Design Peak Wind Effects and Typical Uncertainties

The peak wind effect is a random variable defined as the product of constituent independent random variables, specifically, $p_{pk}(N) = aE_Z K_d G(\theta_m) C_{p,pk}(\theta_m) V^2(N)$. Structural design focuses on the product of the expectations, denoted $\mathbb{E}[p_{pk}(N)] = a\mathbb{E}[E_Z]\mathbb{E}[K_d]\mathbb{E}[G(\theta_m)]\mathbb{E}[C_{p,pk}(\theta_m)]\mathbb{E}[V^2(N)]$, where $\mathbb{E}[\cdot]$ represents expectation. The following expression holds by the multivariate delta method (Casella and Berger 2002, Theorem 5.5.28)

$$\mathbb{E}[p_{pk}(N)] \approx \bar{p}_{pk}(N) = a\bar{E}_z \overline{K}_d \overline{G}(\theta_m) \overline{C}_{p,pk}(\theta_m) \bar{V}^2(N) \quad (1)$$

where $\bar{(\cdot)}$ designates the sample mean or more generally a consistent estimator of the expectation. Appealing to the multivariate delta method a second time yields

$$\mathrm{COV}[\bar{p}_{p,k}(N)] = \{\mathrm{COV}^2[\bar{E}_Z] + \mathrm{COV}^2[\bar{K}_d] + \mathrm{COV}^2[\bar{G}(\theta_m)] + \mathrm{COV}^2[\bar{C}_{p,pk}(\theta_m)] + 4\mathrm{COV}^2[\bar{V}(N)\}^{1/2} \quad (2)$$

In Eq. (1) the factor a = deterministic constant. The aerodynamic coefficient $\bar{C}_{p,pk}(\theta_m)$ depends upon the area being considered. Once this dependence is taken into consideration, for rigid structures the gust response factor $\bar{G} = 1$, and its coefficient of variation $\mathrm{COV}(\bar{G}) = 0$. The mean wind speed with N-year mean recurrence interval (MRI) is denoted $\bar{V}(N)$, and it is estimated from samples of the largest wind speeds regardless of direction; θ_m is the wind direction θ for which the product $\bar{G}(\theta)\bar{C}_{p,pk}(\theta)$ is largest; $\bar{E}_z$ is a terrain exposure factor assumed for simplicity to be independent of direction; z denotes height above the surface; $\bar{K}_d$ is a wind directionality reduction factor that accounts for the fact that the direction θ_m and the directions of the largest directional wind speeds typically do not coincide. For a more complete discussion, see Simiu et al. (2017).

The design peak wind effect with a 50-year MRI may be defined as

$$p_{pk\,des}(N = 50 \text{ years}) = \bar{p}_{pk}(N = 50 \text{ years})\{1 + k\,\mathrm{COV}[\bar{p}_{pk}(N = 50 \text{ years})]\} \quad (3)$$

For codification purposes, the factor k has been determined by calibration with respect to past practice and consensus among expert practitioners; the value $k \approx 2$ (corresponding to the 97.5th percentile of the Gaussian distribution) was adopted after a proposal by Ellingwood et al. (1980, pp. 6–7). The quantity

$$\gamma(N = 50 \text{ years}) \equiv 1 + k\,\mathrm{COV}[\bar{p}_{pk}(N = 50 \text{ years})] \quad (4)$$

is called the wind load factor. Therefore

$$p_{pk\,des}(N = 50 \text{ years}) = \gamma(N = 50 \text{ years})\bar{p}_{pk}(N = 50 \text{ years}) \quad (5)$$

Ellingwood et al. (1980) used $\mathrm{COV}(\bar{E}_z) \approx 0.16$, $\mathrm{COV}(\bar{K}_d) \approx 0$, and $\mathrm{COV}(\bar{G}) \approx 0.11$ for flexible structures. For rigid structures with specified areas, $\mathrm{COV}(\bar{G}) = 0$, as noted earlier. It may further be assumed that, typically, $\mathrm{COV}(\bar{C}_{p,pk}) \approx (0.11^2 + 0.10^2)^{1/2} = 0.15$, where 0.11 is the assumed contribution to the uncertainty due to measurement errors and 0.10 is the assumed contribution due to sampling errors (i.e., to the limited record length). For typical conditions, it is reasonable to assume $\mathrm{COV}[\bar{V}(N = 50 \text{ years})] \approx 0.12$. Justification for these measures of uncertainty can be found in Ellingwood et al. (1980). These values are consistent with those used in the development of the ASCE 7 Standard (ASCE 2005). For rigid structures, they result in a wind load factor $\gamma \approx 1.6$. This value may be used in Eq. (5) in conjunction with the estimated expected peak wind effect if the uncertainties affecting the wind loading do not differ significantly from those underlying the standard. However, measures of uncertainty that differ from those just listed may be used in applications, as appropriate, resulting in wind load factors $\gamma(N = 50 \text{ years})$ that may differ from 1.6. This note considers the case in which the sampling error associated with $\bar{C}_{p,pk}$ is greater than 0.10 due to small sample sizes associated with wind tunnel tests of short duration.

Estimation of $\bar{C}_{p,pk}$ and Its Uncertainty

Estimation of the distribution of the peak aerodynamic coefficient leverages a peaks-over-threshold (POT) stochastic model and Monte Carlo simulation. The full details are described in Duthinh et al. (2017) and summarized here. The wind tunnel history of pressure coefficients is first reversed in sign, if necessary, because the procedure applies only to positive peaks. Next, the time series is declustered to remove the correlation between adjacent observations, a common practice in extreme value analysis. Then, the two-dimensional Poisson process first described for use with extreme values in Pickands (1971) is fitted using maximum likelihood (ML) for a sequence of thresholds. The quality of each fitted model is evaluated using the W-statistic defined in Smith (2004). The threshold providing the highest quality fit is selected as best.

The distribution of $C_{p,pk}$ is empirically constructed using a Monte Carlo approach. That is, a time history of length T_{1m} is generated from the fitted two-dimensional Poisson process using the chosen threshold. The observed maximum of that simulated sample is recorded. That process is repeated many times, say M, and the histogram of the M maximum values estimates the distribution of $C_{p,pk}$. The average of the M maximum values is $\bar{C}_{p,pk}$.

Calculating the uncertainty in the distribution of $C_{p,pk}$ is accomplished using an approximate bootstrap algorithm. Since parameter estimation is done by ML, the negative inverse of the Hessian matrix evaluated at the ML estimate provides information about the uncertainty in the parameter estimates. Thus, the Hessian matrix may be used to randomly perturb the parameter estimates, and the Monte Carlo construction of the distribution of $C_{p,pk}$ is repeated for the perturbed parameter estimates. Repeating the process of perturbing the parameter estimates and constructing a new $C_{p,pk}$ distribution allows uncertainty quantification for any distributional property, most importantly $\bar{C}_{p,pk}$.

Sampling Errors

The POT method described previously is now applied to the time history jp1 of roof corner tap 813 for wind blowing from 315° (0° is parallel to the roof ridge), from the NIST (2004) Aerodynamic Database for Rigid Buildings developed by the University of Western

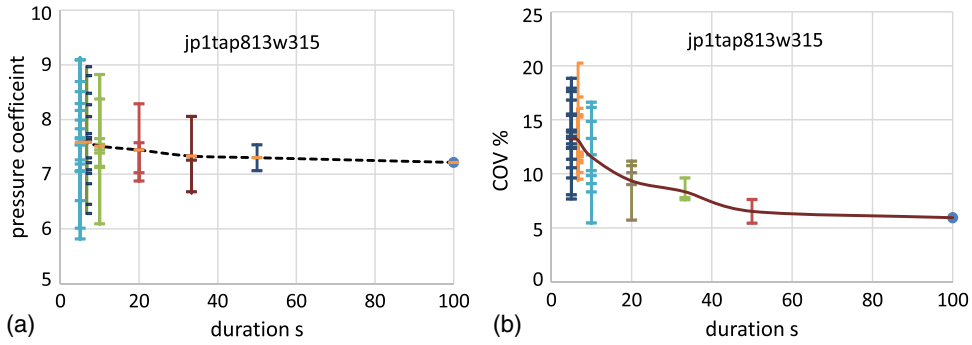

Fig. 1. (a) Means of distributions; and (b) COV of peaks for various test durations, jp1tap813w315, roof corner.

Ontario. The pressure coefficients in the record are referenced to an hourly wind speed at a specified elevation in terrain with the exposure simulated in the wind tunnel tests. The entire time series covers a record duration of 100 s, at 500 Hz, corresponding to a full-scale duration of 60 min. The analysis is performed with the time series divided into n partitions of duration $100/n$ seconds each, with $n = 1, 2, 3, 5, 10, 15$, and 20. For $n = 5$ for example, the analysis of five time-series, each of duration $100/5 = 20$ s yields five estimates (e.g., Duthinh et al. 2017) of the mean of the distribution of the peaks corresponding to a specified duration of 100 s (model scale). These five estimates and their means are plotted in Fig. 1(a). The coefficients of variation (COV in %) associated with these five estimates and the mean of the five COVs are plotted in Fig. 1(b). Similar results are plotted in the same figures for the other values of n, or equivalently, of duration investigated. The means of the peak distributions for various n are connected by a dashed line [Fig. 1(a)], and the means of the COVs are connected by a solid line [Fig. 1(b)]. Two observations are clear from the results: the mean of n estimated means of peak distributions varies little for all values of n investigated; although, individual estimates based on different partitions of the time series corresponding to one value of n have larger variability, indicated by the length of the vertical bars in Fig. 1(a). As expected, the coefficient of variation of the estimated mean of the peak distribution increases as n increases or the duration of the record decreases, as indicated by the length of the vertical bars in Fig. 1(b).

Similar results are obtained for taps 1715 (roof edge), 1712 (roof interior), 2011 (wall interior) and 3905 (wall edge) of Data set jp1 (Building 7, open country) for the most demanding wind directions; and for taps 702 (roof corner), 709 (roof edge), 1712 (roof interior), 2004 (wall interior) and 2201 (wall edge) of Data set eh1 (Data set eh1, Building 15, open country).

Building 7 is 40 ft (12.19 m) wide, 62.5 ft (19.05 m) long, 40 ft high (12.19 m, eave height), and has a roof slope of 1:12 (4.8°). Building 15 is 80 ft (24.38 m) wide, 125 ft (38.10 m) long, 40 ft high (12.19 m, eave height), and has a roof slope of 1:12 (4.8°). Both gable-roofed buildings were modeled at a scale of 1:100, and data were collected for 100 s at 500 Hz.

The plots of these results, together with the locations of the taps and the time series of pressure coefficients, are shown in the Supplemental Data. The taps investigated here are selected in the various roof and wall zones defined by ASCE 7-10. They include the locations that experience the highest wind suction (corners and edges of roof) and the highest positive pressure (center of wall). The observations pertaining to time series jp1tap813w135 apply to the other time series as well.

Load Factor

From Eqs. (2) and (4) and the discussion in the "Design Peak Wind Effects and Typical Uncertainties" section:

$$\gamma(N = 50 \text{ years}) = 1 + k\{\text{COV}^2(\bar{E}_z) + \text{COV}^2(\bar{K}_d) + \text{COV}^2[\bar{G}(\theta_m)] + \text{COV}^2[\bar{C}_{p,pk}(\theta_m)] + 4\text{COV}^2[\bar{V}(N)]\}^{1/2}$$
$$= 1 + 2\{0.16^2 + 0 + 0 + (0.11^2 + \text{SE}^2) + 4 \times 0.12^2\}^{1/2} \quad (6)$$

where SE = sampling error due to the limited sample size of the pressure record.

Tables 1 and 2 list the sampling error and load factor corresponding to various test durations for the time series investigated in Data sets jp1 and eh1, respectively. The number of partitions that the time series are divided into, n, determines the duration of the pressure record. The average COV and the maximum COV are listed for each tap and test duration, and the sampling error selected for calculating the load factor γ [Eq. (6)] is the maximum COV (in *bold*) for that value of n. Due to the dominant presence of other uncertainties in Eq. (6), especially the uncertainty in the square of the wind speed, γ is relatively insensitive to the sampling error in $\bar{C}_{p,pk}$, and thus to the duration of the wind tunnel test. The current load factor $\gamma = 1.6$ can be used for wind tunnel tests lasting about 100 s in model scale, or 60 min in full scale; and $\gamma = 1.7$ (an increase of 6% over 1.6) is implied by the present calculations for wind tunnel tests lasting between 75 and 10 s in model scale, or 45 and 6 min in full scale.

Limitations

These conclusions are based on the investigation of ten time series because this paper focuses on developing a procedure. The reader is cautioned about broadly generalizing these conclusions, especially about drastically decreasing the length of wind tunnel tests without carrying out their own investigation. In the series examined here, the full 100-s series were available for examination. Thus, for $n = 10$, for example, it was possible to argue that the partitions were homogeneous. In contrast, if the partitions were not homogeneous,

Table 1. Sampling error and load factor for various test duration, Data set jp1

	Model scale	Full scale	tap813 w315 roof corner		tap1715w270 roof edge		tap1712w270 roof interior		tap2011w270 wall interior		tap3905 w90 wall edge		
n	duration (s)	duration (min)	Mean COV (%)	Max. COV (%)	Mean COV (%)	Max. COV (%)	Mean COV (%)	Max. COV (%)	Mean COV (%)	Max. COV (%)	Mean COV (%)	Max. COV (%)	γ
1	100	60	5.94	**5.94**	5.53	5.53	5.43	5.43	5.96	5.96	4.48	4.48	1.62
2	50	30	6.52	7.62	9.03	9.92	7.16	7.17	8.09	8.66	10.10	**12.44**	1.67
3	33.33	20	8.34	7.79	5.97	6.64	8.54	9.38	7.62	9.13	10.80	**15.98**	1.70
5	20	12	9.35	11.17	8.11	**11.73**	8.49	10.84	8.56	11.37	9.52	10.39	1.66
10	10	6	11.57	16.63	10.94	**17.96**	9.41	12.45	11.01	13.39	11.91	14.57	1.71
15	6.67	4	13.11	20.24	13.56	**20.11**	10.72	14.38	12.92	17.67	14.24	17.85	1.74
20	5	3	13.24	18.85	14.05	21.66	14.05	20.70	14.43	18.35	14.14	**22.45**	1.76

Note: The average COV and the maximum COV are listed for each tap and test duration, and the sampling error selected for calculating the load factor γ [Eq. (6)] is the maximum COV for that value of n, which is denoted in bold.

Table 2. Sampling error and load factor for various test duration, Data set eh1

	Model scale	Full scale	tap702 w315 roof corner		tap709 w0 roof edge		tap1712w270 roof interior		tap2004w270 wall interior		tap2201w270 wall edge		
n	duration (s)	duration (min)	Mean COV (%)	Max. COV (%)	Mean COV (%)	Max. COV (%)	Mean COV (%)	Max. COV (%)	Mean COV (%)	Max. COV (%)	Mean COV (%)	Max. COV (%)	γ
1	100	60	6.90	6.90	6.31	6.31	3.11	5.11	7.03	7.03	9.18	**9.18**	1.64
2	50	30	7.74	8.96	8.44	9.05	6.43	7.48	8.49	8.81	11.45	**11.78**	1.66
3	33.33	20	9.61	10.81	6.55	9.38	7.82	8.91	10.31	11.25	11.61	**12.28**	1.66
5	20	12	8.69	13.75	9.79	12.27	8.21	9.58	11.01	12.60	11.89	**13.85**	1.68
10	10	6	12.86	19.13	10.65	17.25	10.72	13.27	11.98	16.98	16.48	**20.01**	1.74
15	6.67	4	12.09	17.66	14.44	20.43	10.11	14.52	13.91	18.70	18.63	**24.24**	1.78
20	5	3	13.70	22.27	15.29	22.09	12.14	15.56	14.99	20.79	18.64	**26.90**	1.82

Note: The average COV and the maximum COV are listed for each tap and test duration, and the sampling error selected for calculating the load factor γ [Eq. (6)] is the maximum COV for that value of n, which is denoted in bold.

but differed in some systematic way, those differences would propagate to the $\bar{C}_{p,pk}$. This could happen for example if the partitions were of a shorter duration than the temporal correlation. Such an error would be difficult to diagnose without longer tests.

Conclusion

This paper presents a process for determining how the duration of a wind tunnel test influences the sampling error of the estimated mean of the distribution of the peak wind pressure and, consequently, the estimate of the mean peak pressure and the wind load factor. Due to the dominant presence of other uncertainties, especially wind speed, the load factor changes little over a wide range of test durations. The dominance of the uncertainty attributable to wind speed is due to the fact that in the expression for the wind effects the wind speed is squared. For the series investigated, the current load factor $\gamma = 1.6$ appears reasonable for wind tunnel tests lasting about 100 s in model scale, or 60 min in full scale; $\gamma = 1.7$ (an increase of 6% over 1.6) is found to be sufficient for wind tunnel tests lasting between approximately 75 and 10 s in model scale, or 45 and 6 min in full scale.

Supplemental Data

Figs. S1–S21 are available online in the ASCE Library (www.ascelibrary.org).

References

ASCE. 2005. *Minimum design loads for buildings and other structures*. ASCE/SEI 7-05. Reston, VA: ASCE.

ASCE. 2010. *Minimum design loads for buildings and other structures*. ASCE/SEI 7-10. Reston, VA: ASCE.

Casella, G., and R. L. Berger. 2002. Vol. 2 of *Statistical inference*. 2nd ed. Pacific Grove, CA: Duxbury.

Duthinh, D., A. L. Pintar, and E. Simiu. 2017. "Estimating peaks of stationary random processes: A peaks-over-threshold approach." *ASCE-ASME J. Risk Uncertainty Eng. Syst. Part A Civ. Eng.* 3 (4): 04017028. https://doi.org/10.1061/AJRUA6.0000933.

Ellingwood, B., T. V. Galambos, J. G. MacGregor, and C. A. Cornell. 1980. *Development of a probability based load criterion for American National Standard A58*. NBS SP 577. Washington, DC: National Bureau of Standards.

Minciarelli, F., M. Gioffre, M. Grigoriu, and E. Simiu. 2001. "Estimates of extreme wind effects and wind load factors: Influence of knowledge uncertainties." *Probab. Eng. Mech.* 16 (4): 331–340. https://doi.org/10.1016/S0266-8920(01)00024-8.

NIST. 2004. "Extreme winds and wind effects on structures." Aerodynamic Database for Rigid Buildings. Accessed April 6, 2017. https://www.itl.nist.gov/div898/winds/homepage.htm.

Pickands, J., III. 1971. "The two-dimensional Poisson process and extremal processes." *J. Appl. Probab.* 8 (4): 745–756. https://doi.org/10.2307/3212238.

Rofail, A. W., and K. C. S. Kwok. 1992. "A reliability study of wind tunnel results for cladding pressures." *J. Wind Eng. Ind. Aerodyn.* 44 (1–3): 2413–2424. https://doi.org/10.1016/0167-6105(92)90033-7.

Simiu, E., A. L. Pintar, D. Duthinh, and D. Yeo. 2017. "Wind load factors for use in the wind tunnel procedure." *ASCE-ASME J. Risk Uncertainty Eng. Syst. Part A Civ. Eng.* 3 (4): 04017007. https://doi.org/10.1061/AJRUA6.0000910.

Smith, R. L. 2004. "Statistics of extremes, with applications in environment, insurance, and finance." Chap. 1 in *Extreme values in finance, telecommunications, and the environment*, edited by B. Finkenstädt and H. Rootzén, 1–78. Boca Raton, FL: Chapman & Hall/CRC Press.